

Synthesis and quantum yield investigations of the $\text{Sr}_{1-x-y}\text{Pr}_x\text{Yb}_y\text{F}_{2+x+y}$ luminophores for photonics

S. V. Kuznetsov¹, V. Yu. Proydakova¹, O. A. Morozov², V. G. Gorieva², M. A. Marisov², V. V. Voronov¹,
A. D. Yapryntsev³, V. K. Ivanov³, A. S. Nizamutdinov², V. V. Semashko², P. P. Fedorov¹

¹Prokhorov General Physics Institute, of the Russian Academy of Sciences,
38 Vavilova str., Moscow, 119991 Russia

²Kazan Federal University, 18 Kremlyovskaya, Kazan, 420008 Russia

³Kurnakov Institute of General and Inorganic Chemistry, RAS, 31 Leninsky pr., Moscow, 119991 Russia

kouznetzovsv@gmail.com

DOI 10.17586/2220-8054-2018-9-5-663-668

Single-phase praseodymium- and ytterbium-doped strontium fluoride solid solutions were prepared by co-precipitation from aqueous nitrate solutions followed by annealing at 600 °C. Based on EDX analysis, the content of rare-earth elements in solid phase is slightly higher rather than in initial aqueous solution. All the characteristic praseodymium and ytterbium luminescent bands were present. The most intense luminescence in 800 – 1100 nm range was registered in $\text{SrF}_2:\text{Pr}$ (0.1 mol.):Yb (10.0 mol.%) solid solution. Using the integrating sphere, the values of the quantum yield were estimated. The maximum quantum yield was 1.1 % for $\text{Sr}_{0.9495}\text{Pr}_{0.0005}\text{Yb}_{0.05}\text{F}_{2.0505}$ solid solution.

Keywords: inorganic fluorides, down-conversion luminophores, rare earths, chemical synthesis, photonics, solar cells.

Received: 21 March 2018

Revised: 14 March 2018

1. Introduction

Increasing electric power demand is one of the modern world's challenges [1–3]. The development of alternative sources of electricity, in addition to the use of natural resources, is an urgent task. One of the most advanced approaches is the use of crystalline silicon solar panels. Advantages of these panels are the availability of raw materials the ease of manufacturing, and non-toxicity. One of the major drawbacks is a low efficiency [4,5] due to a limited spectral range of photoresponse, which is located mostly in the near-infrared spectral range with a maximum in the 1 μm region [2]. In the green and red regions of the visible spectrum, crystalline silicon is also photosensitive, but to a lesser extent. There are various approaches to increase the efficiency of converting sunlight to electric power, among which it is worth noting the use of additional fluorescent coatings that convert sunlight into the region of spectral susceptibility of solar cells. It is proposed to use up-conversion phosphors that allow low-energy IR radiation to be transformed to the visible light range, as well as down-conversion phosphors that transform high-energy UV pumping to the luminescence of the visible and near-infrared light range. Among the up-conversion phosphors, one of the most popular compositions is a hexagonal modification of NaYF_4 doped with ytterbium and erbium or ytterbium and thulium [6–9]. Earlier we have proposed another efficient matrix based on strontium fluoride doped with ytterbium and erbium [10–12]. It should also be noted that the quantum yield of up-conversion luminescence is not high and usually stays at the level of few percents. Solid solutions powders based on SrF_2 doped by rare earth elements can be synthesized by different techniques: co-precipitation from aqueous solutions by various fluorinating agents such as HF, NH_4F , KF, NaF [13–15], sol-gel processing in organic solution [16], combustion [17] and hydrothermal synthesis [18–20]. Sol-gel processing in organic solution used gaseous HF, which is very dangerous. Hydrothermal synthesis is also dangerous because of working at high pressures. Combustion product contain typically carbon impurities which result in quenching of luminescence. Luminescence quantum yield for co-precipitation from aqueous solution technique was lower because samples had hydroxyl anion in the crystal structure. The highest luminescence characteristics were attained using ammonium fluoride as fluorinating agent. The existing literature contain only scarce experimental data on the study of solid solutions of $\text{SrF}_2:\text{Yb}:\text{Pr}$ synthesized by co-precipitation from aqueous solutions with ammonium fluoride as fluorination agent. Thus, in this paper, we carried out a complex study of the synthesis and down-conversion luminescent characteristics of $\text{Sr}_{1-x-y}\text{Pr}_x\text{Yb}_y\text{F}_{2+x+y}$ solid solutions.

2. Experimental

We used 99.99 wt% pure ytterbium and praseodymium nitrate hexahydrates, strontium nitrate (LANHIT, Russia), 99.9 % ammonium fluoride (Chimmed, Russia) and doubly-distilled water as the starting materials without further purification. $\text{SrF}_2\text{:Yb:Pr}$ solid solution precipitates were synthesized according to our previously published protocol [12]. Aq. rare earth and strontium nitrate solution of 0.08 M concentration was added dropwise to 7 % excess of 0.16 M aqueous ammonium fluoride under intense stirring. After precipitation of $\text{SrF}_2\text{:Yb:Pr}$ solid solution, the matrix solution was decanted. Precipitates were washed with double distilled water until negative nitrate anion test with diphenylamine. Obtained powders were dried in air at 45 °C (5 hours) and annealed in platinum crucibles in air at 600 °C (1 hour).

All the samples were analyzed by X-ray powder diffraction on a Bruker D8 Advance (Cu $K\alpha$ radiation) diffractometer. Particle size, morphology and composition of the samples were detected using a Carl Zeiss NVision 40 scanning electron microscope equipped with an EDX analyzer. The diffuse reflectance spectra of the samples were recorded using a Lambda 950 Perkin Elmer spectrophotometer. Fluorescence of the samples was excited by a 443 nm cw laser diode (152.8 W/cm²). The luminescence spectra were recorded with Stellarnet EPP 2000 spectrometer using a 5 mm filter (ZhS-16) and corrected for the spectral sensitivity of spectrometer. Quantum yield (QY) in 800 – 1100 nm range was evaluated by integrating sphere upon pumping by a 443 nm cw laser diode (3.567 W/cm²). Experimental data obtained using the integrating sphere was analyzed based approach which described in [21]. Reference calibration lasers (443 nm, 532 nm, 980 nm) were used. In all experiments, the spectral sensitivity of optical systems was calibrated using a SIRSH-2850 lamp.

3. Results

Our earlier studies of $\text{SrF}_2\text{:Yb:Er}$, $\text{SrF}_2\text{:Yb:Tm}$ precipitates confirmed the formation of hydrated solid solutions by co-precipitation from aqueous solution technique [10, 22]. Water and hydroxy-groups can be removed by annealing at 600 °C. Based on this protocol, we synthesized the set of powder samples.

Typical X-ray diffraction pattern of $\text{SrF}_2\text{:Yb:Pr}$ solid solution is presented in Fig. 1. All observed reflections are in a good agreement with JCPDS Card #06-0262 data ($a = 5.800 \text{ \AA}$). XRD results have confirmed that synthesized samples contained the only fluorite-type phase. The lines in X-ray pattern of the sample, dried at 45 °C (Fig. 1a), were much broader than the lines for the sample annealed at 600 °C (Fig. 1b). Thus, annealing at 600 °C leads to increased crystallite size.

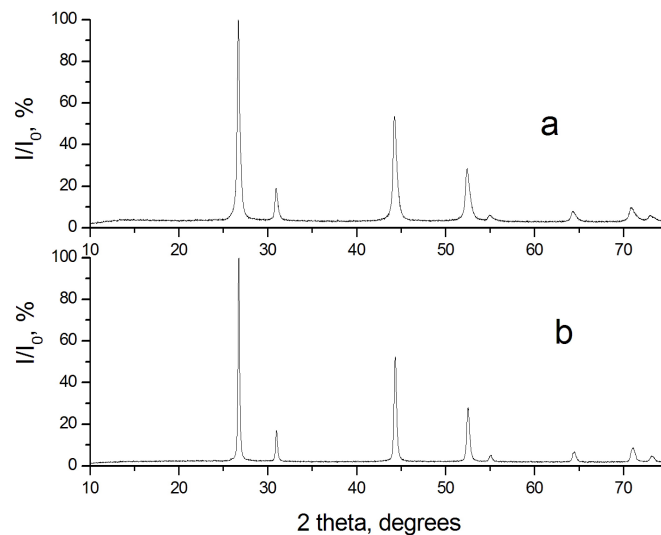


FIG. 1. XRD patterns for sample 3: a – after drying at 45 °C, b – after annealing at 600 °C

We have calculated the unit cell parameters based on XRD data. XRD results are listed in Table 1. Table 1 data analysis also indicate that the increase in the dopant content resulted in the expected simultaneous decrease of $\text{Sr}_{1-x-y}\text{Yb}_x\text{Pr}_y\text{F}_{2+x+y}$ solid solution unit cell parameter due to the action of additional interstitial fluorine ions and smaller ionic radii of the rare earth dopants compared with strontium ion [23]. Annealing at 600 °C also

resulted in expected small decrease in the unit cell parameter in comparison with the data for the same composition samples dried at 45 °C. One of the reason is a smaller ionic radii of fluorine compared to hydroxyl.

TABLE 1. X-Ray diffraction data for $SrF_2:Yb:Pr$ powders

Sample*	Nominal composition, mol. %	T, °C	Unit cell parameter, Å	Weight loss upon annealing (wt. %)
1	$SrF_2: Yb(5.00):Pr(0.05)$	45	$a = 5.789 (2)$	2.84
		600	$a = 5.7821 (4)$	
2	$SrF_2: Yb(5.00):Pr(0.1)$	45	$a = 5.7999 (7)$	5.62
		600	$a = 5.7803 (4)$	
3	$SrF_2: Yb(5.00):Pr(0.5)$	45	$a = 5.789 (1)$	2.60
		600	$a = 5.7790 (6)$	
4	$SrF_2: Yb(10.00):Pr(0.05)$	45	$a = 5.771(3)$	3.8
		600	$a = 5.7637 (2)$	
5	$SrF_2: Yb(10.00):Pr(0.1)$	45	$a = 5.850 (8)$	3.5
		600	$a = 5.746 (2)$	
6	$SrF_2: Yb(10.00):Pr(0.5)$	45	$a = 5.760 (3)$	3.4
		600	$a = 5.7552 (8)$	

*The sample labeling, presented in Table 1, is maintained across the whole paper for the readers convenience

Scanning electron microscopy image of $SrF_2:Yb (5.0\%):Pr (0.5)$ sample dried at 45 °C is shown in Fig. 2a. It appeared to be typical for all the samples. There are two types of particles observed: flat particles with an average size about 14 nm and cubic particles with size about 84 nm. Apparently flat small particles were produced from cubic particles upon milling powder in a mortar which was the preliminary stage for preparing powders for analysis. It is well-known that the alkaline-earth fluorides have perfect cleavage. It results in cracking at mechanical stress. Obviously, in this image we can see with the same situation at nanosized level. One of the arguments is that the ratio of particle sizes complies the $84 \text{ nm}/14 \text{ nm} = 6$. Annealing at 600 °C resulted in an increase of the average particle sizes up to 119 nm (Fig. 2b). As an explanation of the driving forces of such an evolution, it can be assumed that the system is driven to a minimum of its own energy, and also to the destruction of the original self-fluorinating precursor $Sr_{1-x-y-z}Yb_xPr_y(NH_4)_zF_{2+x+y-z}$. In Fig. 2b, SEM image in BSE regime is shown. The uniform color of the image on Fig. 2b revealed a uniform chemical composition of the samples. Evaluation of chemical composition based on EDX measurements is summarized in Table 2. The content of ytterbium fluoride in solid solution is high rather than in water solution. The EDX composition determination error is 0.5 mol.%. This means that the concentration of praseodymium in the samples cannot be determined. Mean value of ytterbium distribution coefficient about 1.15. This means that crystallization process occurs in an incongruent manner.

Diffusion reflectance spectra (Fig. 3) for samples 1, 2, 4 after annealing at 600 °C contained absorption bands typical for praseodymium (III) and ytterbium (III) ions [24]. The intense absorption band of praseodymium is located at 443 nm. Based on this, we have chose 443 nm excitation wavelength.

We have registered the luminescence spectra for annealed samples (Fig. 4). In the visible spectral range, we have recognized characteristic Pr^{3+} ion luminescence in 450 – 750 nm range [25–27] and intense luminescence within 900 – 1100 nm range corresponding to ${}^2F_{5/2} - {}^2F_{7/2}$ transitions of Yb^{3+} ions. The maximum luminescence intensity was recorded for the composition $SrF_2:Pr (0.1 \text{ mol.}\%):Yb (10.0 \text{ mol.}\%)$.

For a more detailed estimation of the down-conversion efficiency we have evaluated the quantum yields of luminescence. There are two main approaches described in many papers. The first is investigation of the lifetime of excited states. This approach appears to be very complicated. The second is the use of the integrating sphere. This approach is more correct, because it consists in registration of a photon flux energy and calculation of quantum yields from the data on energy yields. We have evaluated the quantum yields by means of integrating sphere with

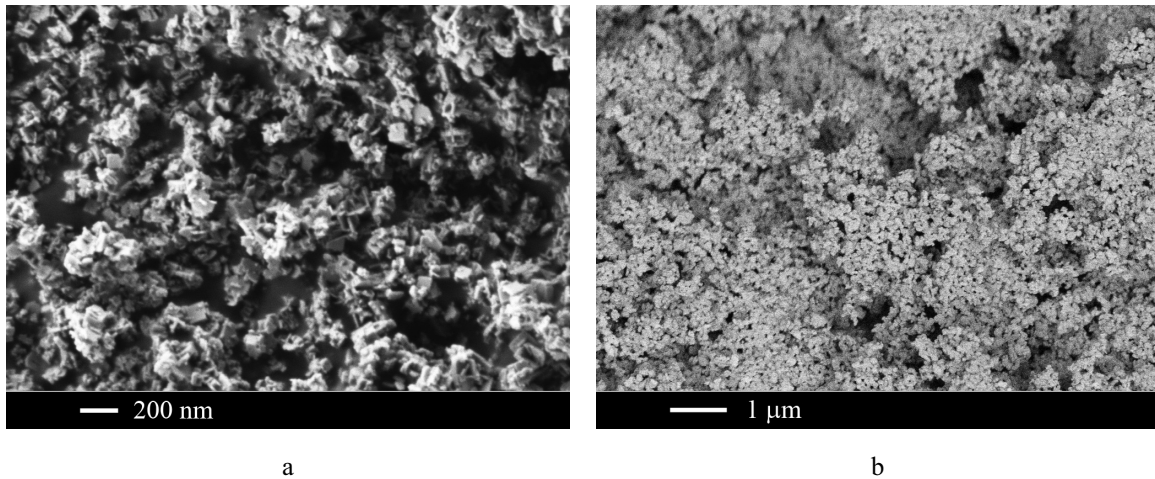


FIG. 2. a – SEM image in SE2 regime of sample 3 after drying at 45 °C, b – SEM image in BSE regime of sample 3 after annealing at 600 °C

TABLE 2. EDX data for SrF₂:Yb:Pr powders

No.	Nominal content Pr/Yb, mol.%	EDX content Pr/Yb, mol.%	The effective distribution coefficient of Yb
1	0.05/5.0	–/5.0	1.0
2	0.10/5.0	–/5.86	1.17
3	0.5/5.0	–/6.0	1.20
4	0.05/10.0	–/12.4	1.24
5	0.10/10.0	–/11.5	1.15

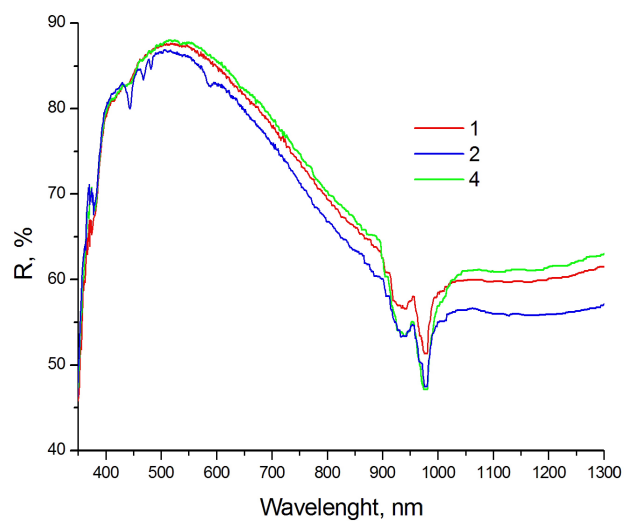


FIG. 3. Diffusion reflection spectra (Fig. 3) for samples 1, 2, 4 after annealing at 600 °C

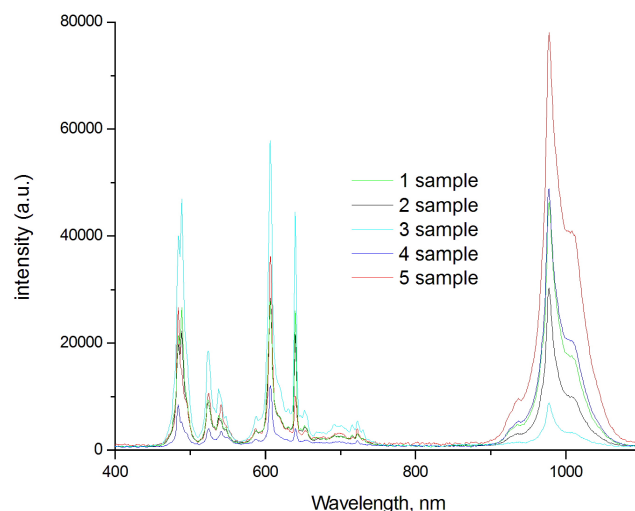


FIG. 4. Luminescence spectra of $Sr_{1-x-y}Pr_xYb_yF_{2+x+y}$ solid solutions after annealing at 600 °C

pumping by a 443 nm cw laser diode with power density 3.567 W/cm² (Table 3). An analysis of the results have showed that at a constant ytterbium content of 5 mol.%, the highest quantum yield is demonstrated by a sample with a praseodymium content of 0.05 mol.%. The increase of praseodymium content by 10 times leads to the quantum yield decrease by 10 times. At the same time, in the samples with 10 mol.% of ytterbium, an increase in the praseodymium content leads to an increase in the quantum yield. As a result, a quantum yield of 1.1 % has been achieved, but further increase of this value with an ytterbium content of 5 mol.% appears to be impossible.

TABLE 3. Quantum yields for $SrF_2:Yb:Pr$ powder samples

No.	Sample composition	Quantum yield, %
1	$SrF_2 : Yb (5 \%) : Pr (0.05)$	1.1
2	$SrF_2 : Yb (5 \%) : Pr (0.1)$	0.7
3	$SrF_2 : Yb (5 \%) : Pr (0.5)$	0.1
4	$SrF_2 : Yb (10 \%) : Pr (0.05)$	0.5
5	$SrF_2 : Yb (10 \%) : Pr (0.1)$	0.8

4. Conclusions

As a result of the study, single-phase samples of $Sr_{1-x-y}Pr_xYb_yF_{2+x+y}$ solid solutions were obtained, which was confirmed by XRD, SEM, and EDX measurements. The shape of the particles dried at 45 °C is cubic of about 84 nm in size and a plate-like with a thickness of 14 nm, which is probably the result of splitting the cubes along the cleavage planes. Annealing at 600 °C leads to a change in the size and the morphology of the particles. In this case, spheres with the size of 119 nm appear. It should be noted that particles do not tend to agglomeration. EDX analysis have shown that the ytterbium concentration in solid solutions is greater than in the initial aqueous solutions. The effective average distribution coefficient was 1.15, which indicates the incongruent type of the precipitation process from aqueous solutions. The diffuse reflectance spectra contain characteristic absorption bands of praseodymium and ytterbium, which confirms their entry into the crystal lattice. Considering the fact that the maximum photoconversion of solar power in crystalline silicon is attained in the region of 1 μ m, the best composition determined on the basis on the quantum yield measurements is $SrF_2: Yb(5.00): Pr(0.05)$ solid solution with QY = 1.1 %.

Acknowledgement

The study was funded by a grant from the Russian Science Foundation (project # 17-73-20352).

References

- [1] Green M.A., Bremner S.P. Energy conversion approaches and materials for high-efficiency photovoltaics. *Nature Mater.*, 2017, **16**, P. 23–34.
- [2] Huang X., Han S., Huang W., Liu X. Enhancing solar cell efficiency: the search for luminescent materials as spectral converters. *Chem. Soc. Rev.*, 2013, **42**, P. 173–201.
- [3] Han G., Zhang S., Boix P.P., Wong L.H., Sun L., Lien S.Y. Towards high efficiency thin film solar cells. *Progress in Materials Science*, 2017, **87**, P. 246–291.
- [4] Engelhart P., Wendt J., Schulze A., Klenke C., Mohr A., Petter K., Stenzel F., Hörmlein S., Kauert M., Junghänel M., Barkenfeld B., Schmidt S., Rychtarik D., Fischer M., Müller J.W., Wawer P. R&D pilot line production of multi-crystalline Si solar cells exceeding cell efficiencies of 18 %. *Energy Procedia*, 2011, **8**, P. 313–317.
- [5] Yang J., Myong S.Y., Lim K.S. Novel ultrathin LiF interlayers for efficient light harvesting in thin-film Si tandem solar cells. *Solar Energy*, 2015, **114**, P. 259–267.
- [6] Ren W., Tian G., Jian S., Gu Z., Zhou L., Yan L., Jin S., Yin W., Zhao Y. Tween coated NaYF₄:Yb,Er/NaYF₄ core/shell upconversion nanoparticles for bioimaging and drug delivery. *RSC Advances*, 2012, **2**, P. 7037–7041.
- [7] Zhao J., Jin D., Scharfner E.P., Lu Y., Liu Y., Zvyagin A.V., Zhang L., Dawes J.M., Xi P., Piper J.A., Goldys E.M., Monro T.M. Single-nanocrystal sensitivity achieved by enhanced upconversion luminescence. *Nature Nanotechnology*, 2013, **8**, P. 729–734.
- [8] Conference book of 1st Conference and spring school on properties, design and applications of upconverting nanomaterials, Wroclaw, Poland, 23-27 May 2016.
- [9] Kuznetsov S.V., Yasyrkina D.S., Ryabova A.V., Pominova D.V., Voronov V.V., Baranchikov A.E., Ivanov V.K., Fedorov P.P. α -NaYF₄:Yb:Er@AlPc(C₂O₃)₄ -based efficient up-conversion luminophores capable to generate singlet oxygen under IR excitation. *J. Fluor. Chem.*, 2016, **182**, P. 104–108.
- [10] Pak A.M., Ermakova J.A., Kuznetsov S.V., Ryabova A.V., Pominova D.V., Voronov V.V. Efficient visible range SrF₂:Yb:Er- and SrF₂:Yb:Tm-based up-conversion luminophores. *J. Fluor. Chem.*, 2017, **194**, P. 16–22.
- [11] Rozhnova Yu.A., Luginina A.A., Voronov V.V., Ermakov R.P., Kuznetsov S.V., Ryabova A.V., Pominova D.V., Arbenina V.V., Osiko V.V., Fedorov P.P. White light luminophores based on Yb³⁺/Er³⁺/Tm³⁺-coactivated strontium fluoride powders. *Mater. Chem. Phys.*, 2014, **148**, P. 201–207.
- [12] Rozhnova Yu.A., Kuznetsov S.V., Luginina A.A., Voronov V.V., Ryabova A.V., Pominova D.V., Ermakov R.P., Usachev V.A., Kononenko N.E., Baranchikov A.E., Ivanov V.K., Fedorov P.P. New Sr_{1-x-y}R_x(NH₄)_yF_{2+x-y} (R = Yb, Er) solid solution as precursor for high efficiency up-conversion luminophor and optical ceramics on the base of strontium fluoride. *Mater. Chem. Phys.*, 2016, **172**, P. 150–157.
- [13] Fedorov P.P., Kuznetsov S.V., Mayakova M.N., Voronov V.V., Ermakov R.P., Baranchikov A.E., Osiko V.V. Coprecipitation from aqueous solutions to prepare binary fluorides. *Rus. J. Inorg. Chem.*, 2011, **56**, P. 1525–1531.
- [14] Mayakova M.N., Luginina A.A., Kuznetsov S.V., Voronov V.V., Ermakov R.P., Baranchikov A.E., Ivanov V.K., Karban O.V., Fedorov P.P. Synthesis of SrF₂-YF₃ nanopowders by co-precipitation from aqueous solutions. *Mendeleev Communications*, 2014, **24**, P. 360–362.
- [15] Fedorov P.P., Mayakova M.N., Maslov V.A., Baranchikov A.E., Ivanov V.K., Pynenkov A.A., Uslamina M.A., Nishchev K.N. The solubility of sodium and potassium fluorides in the strontium fluoride. *Nanosystems: PHYSICS, CHEMISTRY, MATHEMATICS*, 2017, **8**, P. 830–834.
- [16] Ritter B., Haida P., Krahl T., Scholz G., Kemnitz E. Core-shell metal fluoride nanoparticles via fluorolytic sol-gel synthesis – a fast and efficient construction kit. *J. Mater. Chem.*, 2017, **C5**, P. 5444–5450.
- [17] Rakov N., Guimarães R.B., Franceschini D.F., Maciel G.S. Er:SrF₂ luminescent powders prepared by combustion synthesis. *Mater. Chem. Phys.*, 2012, **135**, P. 317–321.
- [18] Peng J., Hou S., Liu X., Feng J., Yu X., Xing Y., Su Z. Hydrothermal synthesis and luminescence properties of hierarchical SrF₂ and SrF₂:Ln³⁺ (Ln = Er, Nd, Yb, Eu, Tb) micro/nanocomposite architectures. *Mater. Res. Bull.*, 2012, **47**, P. 328–332.
- [19] Yagoub M.Y.A., Swart H.C., Noto L.L., O’Connell J.H., Lee M.E., Coetsee E. The effects of Eu-concentrations on the luminescent properties of SrF₂:Eu nanophosphor. *J. Lumin.*, 2014, **156**, P. 150–156.
- [20] Yagoub M.Y.A., Swart H.C., Noto L.L., Bergman P., Coetsee E. Surface Characterization and Photoluminescence Properties of Ce³⁺, Eu Co-Doped SrF₂ Nanophosphor. *Materials*, 2015, **8**, P. 2361–2375.
- [21] Ryabova A.V., Pominova D.V., Krut’ko V.A., Komova M.G., Loschenov V.B. Spectroscopic research of upconversion nanomaterials based on complex oxide compounds doped with rare-earth ion pairs: benefit for cancer diagnostics by upconversion fluorescence and radiosensitive methods. *Photonics&Lasers in Medicine*, 2013, **2**, P. 117–128.
- [22] Kuznetsov S., Ermakova Yu., Voronov V., Fedorov P., Busko D., Howard I.A., Richards B., Turshatov A. Up-conversion Quantum Yield of SrF₂:Yb³⁺,Er³⁺ Sub-micron Particles Prepared by Precipitation from Aqueous Solution. *J. Mater. Chem.*, 2018, **C6**, P. 598–604.
- [23] Fedorov P.P., Sobolev B.P. Concentration dependence of unit-cell parameters of phases M_{1-x}R_xF_{2+x} with the fluorite structure. *Sov. Phys. Crystallogr.*, 1992, **37**, P. 651–656.
- [24] Dieke G.H., Crosswhite H.M. The spectra of the doubly and triply ionized rare earths. *Appl. Opt.*, 1963, **2**, P. 675–686.
- [25] Kuzmanoski A., Pankratov V., Feldmann C. Energy transfer of the quantum-cutter couple Pr³⁺-Mn²⁺ in CaF₂:Pr³⁺, Mn²⁺ nanoparticles. *J. Lumin.*, 2016, **179**, P. 555–561.
- [26] Meijerink A., Wegh R., Vergeer P., Vlucht T. Photon management with lanthanides. *Opt. Mater.*, 2006, **28**, P. 575–581.
- [27] Yagoub M.Y.A., Swart H.C., Coetsee E. Concentration quenching, surface and spectral analyses of SrF₂:Pr³⁺ prepared by different synthesis techniques. *Opt. Mater.*, 2015, **42**, P. 204–209.